

# Surface brightness profiles and structural parameters for 10 rich stellar clusters in the Small Magellanic Cloud

A. D. Mackey<sup>1\*</sup> and G. F. Gilmore<sup>1</sup>

<sup>1</sup>*Institute of Astronomy, University of Cambridge, Madingley Road, Cambridge CB3 0HA*

Accepted – Received –

## ABSTRACT

As a follow up to our recent study of a large sample of LMC clusters (Mackey & Gilmore 2002), we have conducted a similar study of the structures of ten SMC clusters, using archival *Hubble Space Telescope* snapshot data. We present surface brightness profiles for each cluster, and derive structural parameters, including core radii and luminosity and mass estimates, using exactly the same procedure as for the LMC sample.

Because of the small sample size, the SMC results are not as detailed as for the larger LMC sample. We do not observe any post core-collapse clusters (although we did not expect to), and there is little evidence for any double clusters in our sample. Nonetheless, despite the small sample size, we show for the first time that the SMC clusters follow almost exactly the trend in core radius with age observed for the LMC system, including the apparent bifurcation at several hundred Myr. This further strengthens our argument that this relationship represents true physical evolution in these clusters, with some developing significantly expanded cores due to an as yet unidentified physical process. Additional data, both observational and from *N*-body simulations, is still required to clarify many issues.

**Key words:** galaxies: star clusters – Magellanic Clouds – globular clusters: general – stars: statistics

## 1 INTRODUCTION

We recently conducted a study of the structures of a large sample of rich star clusters in the Large Magellanic Cloud (LMC) (Mackey & Gilmore 2002; hereafter Paper I), in which we compiled a pseudo-snapshot data set from the *Hubble Space Telescope* (*HST*) archive and used these observations to construct high resolution surface brightness profiles. From these profiles, we were able to obtain measurements of the structural parameters of each cluster, including their core radii, and total luminosities and masses. We also demonstrated that these clusters followed a trend in core radius with age – namely that the spread in core radius increases significantly as the clusters grow older, a result previously discussed by Elson and collaborators (Elson et al. 1989; Elson 1991; Elson 1992). It seems likely that this trend reflects real physical evolution of these clusters, as argued in Paper I, although the mechanism by which the cores of some clusters expand during their lifetimes while the cores of others do not, is as yet unidentified. We are currently carrying out *N*-body simulations to investigate in detail several physical processes which might drive core expansion (e.g., Wilkinson et al., in prep.).

Having exhausted the suitable archival LMC data, we now turn our attention to the cluster system in the Small Magellanic Cloud (SMC). The SMC cluster system is similar to that of the

LMC in that it contains rich star clusters of masses comparable to Galactic globular clusters, and with ages spanning the range  $10^6 - 10^{10}$  yr. The two systems however, have dissimilar cluster formation histories and age-metallicity relationships (see e.g., Rich et al. (2001), for a brief review). The number of SMC clusters is also far fewer than the number of clusters in the LMC, and the SMC system has been far less extensively studied. It is not surprising then that there are few available surface brightness profiles for SMC clusters, and (prior to the present study) it was not known whether the SMC cluster system followed the core radius vs. age relationship observed for LMC clusters. In fact, we were only able to locate in the literature three low resolution density profile studies from photographic plates – those of Kontizas, Danezis & Kontizas (1982), Kontizas & Kontizas (1983), and Kontizas, Theodossiou & Kontizas (1986).

It therefore seemed very worthwhile to extract what archival *HST* frames we could locate, and reduce these using the same procedure we had applied to the LMC sample, so that we now have two directly comparable and entirely homogeneous data sets. We describe these data in Section 2 and briefly reiterate the reduction process in Section 3 – this process and the problems and uncertainties associated with it have been described in great detail in Paper I. We present the surface brightness profiles and the derivation of key structural parameters in Section 4, and a discussion of these results in the context of the core radius vs. age trend in Section 5. The results from the present study (Tables 1, 2, 3, and 5) to-

\* E-mail: dmackey@ast.cam.ac.uk

gether with the surface brightness profiles, are available on-line at [http://www.ast.cam.ac.uk/STELLARPOPS/SMC\\_clusters/](http://www.ast.cam.ac.uk/STELLARPOPS/SMC_clusters/).

## 2 THE CLUSTER SAMPLE

### 2.1 Observations

Just as for the LMC cluster sample, the observational basis of this project is archival *HST* data, again from *HST* project 5475 which was a Wide Field Planetary Camera 2 (WFPC2) snapshot survey of Magellanic Cloud clusters. The data consists of two WFPC2 exposures per field, with the F450W and F555W filters respectively. Exposure times span the ranges 80–600 s in F450W and 40–300 s in F555W, with the observation dates between 1994 January 26 and 1995 January 21. Around half of the SMC cluster exposures were taken before the WFPC2 cool-down of 1994 April 23.

Although thirteen clusters were targeted by this survey, we accepted only ten for reduction. The observations of NGC 422 were of poor data quality, and those for NGC 465 did not have a rich cluster suitable for the construction of a surface brightness profile in the field of view. As noted by Crowl et al. (2001), the observation labelled as NGC 419 is in fact a duplicate observation of NGC 411, at a different roll angle. Exclusion of these three observations left a homogeneous sample of ten, which are listed in Table 1 along with their observation details. Unlike with the LMC sample, we were not able to extend the current sample by including additional archival data – no suitable observations could be located.

We note however, the existence of additional imaging of NGC 121 and NGC 330 in the *HST* archive. In the interests of maintaining consistency with our LMC data and our established reduction procedure, we chose not to use these observations. Paper I contains a full discussion of the existence of extra archival data, and the reasons for its non-use.

### 2.2 Literature data

We have compiled literature data for the identifiers, positions, ages and metallicities of the ten clusters in the present sample. These data are presented in Table 2. Like for the previous LMC sample, we have tried to make this compilation as homogeneous as possible, which means taking the results of larger scale studies where possible, but without sacrificing the quality of the data by neglecting other high resolution or high accuracy measurements. As with the compilation in Paper I, this compilation is not intended to be an exhaustive survey of the available literature; rather it merely provides a consistent set of age and metallicity estimates as a reference point for this and future work.

#### 2.2.1 Cluster names and positions

We have taken the most common identifiers for each cluster from the Simbad Astronomical Database (<http://simbad.u-strasbg.fr/>). In all but one case the principal designation is an NGC number, with the other labels (in parenthesis) being drawn from the catalogues of Kron (1956) (Kron) and Lindsay (1958) (Lindsay; abbreviated to ‘L’ in tables and figures). Positions are taken from Welch (1991), precessed to J2000.0, except that for NGC 121 which is from Simbad. Although we later derive considerably more precise positions, none of these are significantly different from the literature values described here. We have also listed the projected angular distance  $R_{opt}$  to the optical centre of the SMC at  $\alpha = 00^h52^m45^s$ ,

$\delta = -72^\circ49'43''$  (J2000.0) (Westerlund 1997). Because the SMC has a complex disrupted structure, its rotation centre (and rotation curve) are not easily derived and remain the subject of debate (Westerlund 1997). We therefore do not quote projected angular distances from a rotation centre here, but consider this further in Section 5, below.

#### 2.2.2 Cluster ages

The SMC cluster system is less extensively studied than the LMC system, and age determinations based on colour-magnitude diagrams (CMDs) from CCD measurements are correspondingly sparse. We have adopted the majority of our ages from the analysis of Mighell, Sarajedini & French (1998), who determine CMDs for five of the clusters in the present sample (NGC 121, NGC 339, NGC 361, NGC 416, and Kron 3) from exactly the same archival *HST* snapshot data. We take the ages of NGC 152 and NGC 411 from Crowl et al. (2001) and Alves & Sarajedini (1999) respectively, with these two studies using similar analysis techniques to those of Mighell et al. Rich et al. (2000) have published a separate analysis of the same archival data using a different age determination technique, and find NGC 152 and NGC 411 to be coeval ( $\tau = 2 \pm 0.5$  Gyr) and NGC 339, NGC 361, NGC 416 and Kron 3 to be coeval ( $\tau = 8 \pm 2$  Gyr). Both results are consistent within the errors with the ages adopted from the three studies listed above. For NGC 330, we take an age estimate from the study of Chiosi et al. (1995); see also the discussion of Da Costa & Hatzidimitriou (1998). Da Costa & Hatzidimitriou also discuss literature estimates for the age of NGC 458 and we take the average of the two values mentioned in this discussion. Finally, for NGC 176 we resort to the photographic plate photometry of Hodge & Flower (1987) who suggest an age of  $\sim 0.4$  Gyr. However, our unpublished CMD suggests an age much more similar to that of NGC 458 or younger, so we adopt  $\tau \sim 0.2$  Gyr, but with large error-bars to cover both possibilities.

#### 2.2.3 Cluster metallicities

Literature estimates for SMC cluster metallicities are also few and far between. To maintain consistency, we have adopted the cluster metallicities determined in conjunction with their ages by Mighell et al. (1998) for NGC 121, NGC 339, NGC 361, NGC 416, and Kron 3, by Alves & Sarajedini (1999) for NGC 411, and by Crowl et al. (2001) for NGC 152. In each of these cases, the uncertainties we quote are those formally derived by the authors, and represent the uncertainties from both their data and their fitting procedures. Da Costa & Hatzidimitriou (1998) have measured spectroscopic abundances based on the calcium triplet for three of these clusters – NGC 121, NGC 339, and Kron 3. Their age-corrected results show good consistency with the values adopted here for these three clusters. For NGC 330, we take the metallicity determined from the high resolution spectroscopy of Hill (1999), and for NGC 458 the metallicity estimated from the literature by Da Costa & Hatzidimitriou. Finally, for NGC 176 we could not locate any suitable metallicity measurements, so we have used the SMC age-metallicity relationship presented by Da Costa & Hatzidimitriou to estimate  $[\text{Fe}/\text{H}] \sim -0.6$ . This final metallicity is not intended as anything more than a crude estimate, and we adopt it solely for the purpose of estimating mass to light ratios later in the analysis. In Paper I we showed that these calculations are relatively insensitive to the selected metallicity, so we are confident in using the metallic-

**Table 1.** Cluster list and observation details.

Cluster Name	Program ID	Principal Frame				Secondary Frame			
		Filter	Data set	Date	Time (s)	Filter	Data set	Date	Time (s)
NGC121	5475	F555W	u26m0102t	26/01/1994	300	F450W	u26m0101t	26/01/1994	600
NGC152	5475	F555W	u26m0702t	26/09/1994	160	F450W	u26m0701t	26/09/1994	300
NGC176	5475	F555W	u26m0802t	21/01/1995	100	F450W	u26m0801t	21/01/1995	200
NGC330	5475	F555W	u26m0b02t	27/01/1994	40	F450W	u26m0b01t	27/01/1994	80
NGC339	5475	F555W	u26m0202t	07/04/1994	200	F450W	u26m0201t	07/04/1994	400
NGC361	5475	F555W	u26m0602t	03/04/1994	160	F450W	u26m0601t	03/04/1994	300
NGC411	5475	F555W	u26m0402t	24/05/1994	200	F450W	u26m0401t	24/05/1994	400
NGC416	5475	F555W	u26m0502t	06/02/1994	200	F450W	u26m0501t	06/02/1994	400
NGC458	5475	F555W	u26m0a02t	03/02/1994	40	F450W	u26m0a01t	03/02/1994	80
KRON3	5475	F555W	u26m0g02t	27/05/1994	300	F450W	u26m0g01t	27/05/1994	600

**Table 2.** Literature nomenclature, position, age and metallicity data for the cluster sample.

Principal Name	Alternative Names	Position (J2000.0)			$R_{opt}$ ( $^{\circ}$ ) <sup>a</sup>	$\log \tau$ (yr)	Age Ref.	Metallicity [Fe/H]	Met. Ref.
		$\alpha$	$\delta$						
NGC121	KRON2, L10	$00^h 26^m 49^s$	$-71^{\circ} 32' 10''$	2.43	$10.08 \pm 0.05$	7	$-1.71 \pm 0.10$	7	
NGC152	KRON10, L15	$00^h 32^m 56^s$	$-73^{\circ} 06' 59''$	1.47	$9.15^{+0.06}_{-0.07}$	3	$-0.94 \pm 0.15$	3	
NGC176	KRON12, L16	$00^h 35^m 59^s$	$-73^{\circ} 09' 57''$	1.26	$8.30^{+0.30}_{-0.30}$	6, 8	$\sim -0.6$	*	
NGC330	KRON35, L54	$00^h 56^m 20^s$	$-72^{\circ} 27' 44''$	0.46	$7.40^{+0.20}_{-0.40}$	2, 4	$-0.82 \pm 0.11$	5	
NGC339	KRON36, L59	$00^h 57^m 45^s$	$-74^{\circ} 28' 21''$	1.68	$9.80^{+0.08}_{-0.10}$	7	$-1.50 \pm 0.14$	7	
NGC361	KRON46, L67	$01^h 02^m 11^s$	$-71^{\circ} 36' 25''$	1.43	$9.91^{+0.06}_{-0.07}$	7	$-1.45 \pm 0.11$	7	
NGC411	KRON60, L82	$01^h 07^m 56^s$	$-71^{\circ} 46' 09''$	1.59	$9.15^{+0.06}_{-0.07}$	1, 3	$-0.68 \pm 0.07$	1, 3	
NGC416	KRON59, L83	$01^h 07^m 58^s$	$-72^{\circ} 21' 25''$	1.25	$9.84^{+0.06}_{-0.08}$	7	$-1.44 \pm 0.12$	7	
NGC458	KRON69, L96	$01^h 14^m 54^s$	$-71^{\circ} 32' 58''$	2.17	$8.30^{+0.18}_{-0.30}$	4	$-0.23^{+0.1}_{-0.4}$	4	
KRON3	L8	$00^h 24^m 46^s$	$-72^{\circ} 47' 37''$	2.07	$9.78^{+0.09}_{-0.11}$	7	$-1.16 \pm 0.09$	7	

Reference list: 1. Alves & Sarajedini (1999); 2. Chiosi et al. (1995); 3. Crowl et al. (2001); 4. Da Costa & Hatzidimitriou (1998); 5. Hill (1999); 6. Hodge & Flower (1987); 7. Mighell et al. (1998); 8. This paper.

\* Calculated metallicity, as described in the text.

<sup>a</sup> Relative to the optical centre of the SMC, at  $\alpha = 00^h 52^m 45^s$ ,  $\delta = -72^{\circ} 49' 43''$  (J2000.0) (Westerlund 1997)

ity for NGC 176 in this case. Any subsequent use must be carefully judged on the nature of the calculation at hand.

### 3 PHOTOMETRY AND SURFACE BRIGHTNESS PROFILES

The data reduction, photometry, and construction of surface brightness profiles followed exactly the procedures outlined in Paper I, and for a detailed description we refer the reader to this paper. For completeness, we provide a much-abbreviated summary below.

As part of the retrieval process, all archival exposures are reduced according to the standard *HST* pipeline, using the latest available calibrations. We used the HSTphot software package (Dolphin 2000a), and in particular the *multi*phot routine, to make our photometric measurements from the reduced frames. HSTphot is tailored for WFPC2 observations, accounting in detail for the severely under-sampled PC/WFC point spread functions (PSFs) and the four chip structure of the camera. The images were first cleaned<sup>†</sup> using the packages provided with HSTphot, and then the photometry

performed using HSTphot in PSF fitting mode, with a minimum detection threshold of  $3\sigma$  above the local background. Parameters derived during the PSF fitting routines, such as the object classification, sharpness parameter, and goodness-of-fit parameter  $\chi$  helped clean the photometry of spurious detections and non-stellar objects. We selected only stellar classified objects with sharpnesses in the interval  $[-0.6, +0.6]$  and  $\chi \leq 3.5$ , which provided a perfectly adequate selection for the purposes of constructing surface brightness profiles. Photometry for these selected objects was corrected for geometric distortion, filter-dependent plate scale changes, and the CCD 34th row errors. Finally, charge-transfer efficiency (CTE) effects were corrected using the calibration of Dolphin (2000b), PSF residuals accounted for, and the final measurements corrected to an aperture of  $0''.5$  and the zero-points of Dolphin (2000b).

For each cluster, the selections of measured stars were used to independently construct two surface brightness profiles – one for each colour. Comparison of each pair of profiles provided a good consistency check. The difficulties associated with constructing profiles from WFPC2 observations are outlined in Paper I; here

<sup>†</sup> i.e., the masking of bad regions and pixels, a first attempt at removing

cosmic rays and hot and saturated pixels, and the robust determination of a background image.

we simply summarize our procedure. First, the chip and pixel coordinates for each star are converted to corrected pixel coordinates relative to the WFC2 chip, using the IRAF STSDAS task METRIC. This procedure does not use any image header information, so the inaccuracies which sometimes occur in image headers are circumvented. Next, the centre of each cluster (or more correctly, the surface brightness peak of a cluster) is located using a simple Monte Carlo style algorithm. Accuracy in the centre determination is vital, since poor centering will tend to artificially flatten a surface brightness profile, which will cause systematic errors in the determination of structural parameters. Our algorithm is repeatable typically to  $\pm 10$  WFC pixels, or approximately  $\pm 1''$ .

Four sets of annuli are then generated about the centre. Two sets are of narrow width ( $1''.5$  and  $2''$ , extending to  $\sim 20''$  and  $\sim 30''$  respectively) and are designed for sampling of the core, while the other two sets are wider ( $3''$  and  $4''$ , both extending as far as possible) and are designed for sampling the outer regions. The surface brightness  $\mu_i$  of the  $i$ -th annulus in a set is found simply by counting the stars which fall in that annulus, so that

$$\mu_i = \frac{A_i}{\pi(b_i^2 - a_i^2)} \sum_{j=1}^{N_s} C_j F_j \quad (1)$$

where  $b_i$  and  $a_i$  are the outer and inner radii of the annulus respectively,  $N_s$  is the number of stars in the annulus, and  $F_j$  is the flux of the  $j$ -th star. The factors  $A_i$  and  $C_j$  are the area correction for an annulus and the completeness correction for a star respectively, and must be determined before the annulus is constructed.

The area correction for an annulus is designed to ensure the surface brightness is normalized to that for a complete annulus – this is necessary because the shape of the WFPC2 camera and the arbitrary cluster centering and observation roll-angle mean that most annuli about the cluster centre are not fully imaged. If this factor was not accounted for, serious artificial fluctuations would evidently be introduced into each profile. Because of the complicated observation geometries, analytic determination of each area correction is overly difficult; rather, we determined them numerically, as outlined in Paper I. Annuli with  $A_i > 3$  are not used – this limits the maximum profile radius to  $\sim 75 - 80''$ , depending on the position of the cluster centre on the camera.

The completeness correction for a star is designed to account for those stars missed by the detection software due to faintness and crowding. We used the artificial star routine attached to *multiplot* in the manner described in Paper I, to develop a stellar completeness function which is dependent on chip and pixel coordinates, magnitude, and colour. This function is in the form of a look-up table, so the appropriate correction for the  $j$ -th star may be easily located according to the star's properties. Stars with  $C_j > 4$  were discarded to avoid introducing large random errors. Unlike several of the clusters in the larger LMC sample, none of the clusters in the present sample suffered from serious crowding or saturation, so the completeness corrections were usually small, and the positional binning resolution described in Paper I was always perfectly adequate. In addition, there was never a need for extra data from short exposures (see Paper I) to be introduced.

Just as with most of the LMC clusters in Paper I, saturated stars were also not a problem. Only one of the clusters in the present sample – the very young cluster NGC 330 – had significant numbers of saturated stars ( $\gtrsim 10$ ) within approximately two core radii. This cluster appears similar to the young LMC clusters NGC 1805 and NGC 1818, which suffered similar numbers of saturated stars in the measurements made in Paper I. In the LMC case, we demon-

strated that it made sense to leave such stars (predominantly very short lived giants and upper main sequence stars) out of the surface brightness profile construction, in order to measure properly the underlying stellar distribution. The case of NGC 330 is exactly similar and we are therefore confident in leaving the saturated stars from this cluster out of any further calculations.

The internal errors  $\sigma_i$  for each annulus were determined initially according to the method outlined by Djorgovski (1987) – that is, each annulus was divided into eight and the standard deviation of the segmental surface brightnesses taken to be the error. As described in Paper I, this worked well in the inner regions of a cluster but broke down in the outer regions, badly underestimating the scatter. Therefore, after the background subtraction but before the final model fit (see below), we calculated the Poisson errors for each annulus, and in the cases where these were significantly larger than the original errors we substituted the new errors instead. For some clusters, particularly those of low density, both the Poisson and sector errors are larger than the RMS point-to-point scatter. This is a consequence of the calculation technique and is addressed at length in Paper I (Section 4.2.5).

EFF models (after Elson, Fall & Freeman (1987)) of the form

$$\mu(r) = \mu_0 \left( 1 + \frac{r^2}{a^2} \right)^{-\frac{\gamma}{2}} \quad (2)$$

were fit to each profile, where  $\mu_0$  is the central surface brightness,  $a$  is a measure of the core radius and  $\gamma$  is the power-law slope at large radii. These profiles are essentially the same as the family of empirical King (1962) models, without tidal truncation. The parameter  $a$  is related to the usual King core radius  $r_c$  by

$$r_c = a(2^{2/\gamma} - 1)^{1/2} \quad (3)$$

provided the tidal cut-off  $r_t \gg r_c$ ; a safe assumption for most of the clusters in this sample, given the relatively weak tidal field of the SMC.

The fitting of these profiles was achieved using weighted least-squares minimization on an adaptive grid, as described in Paper I. Because many of the clusters lie in well-populated regions of the SMC, field star contamination needed to be corrected for. This was done by initially fitting an EFF model to the central region of a profile, where field contamination is not significant. This provided estimates of the parameters  $\mu_0$  and  $r_c$ , which were subsequently used to fit, in the outer regions of the profile, a model of the form:

$$\begin{aligned} \mu(r) &\approx \mu_0 \left( \frac{r}{a} \right)^{-\gamma} + \phi \\ &\approx \mu_0 \left( \frac{r}{r_c} \right)^{-\gamma} (2^{2/\gamma} - 1)^{-\gamma/2} + \phi \end{aligned} \quad (4)$$

which is Eq. 2 with  $r \gg a$ , a flat background contribution  $\phi$ , and Eq. 3 substituted. From this model we determined  $(\gamma, \phi)$ , so that the field contamination level could be subtracted from each annulus in the profile. Finally, an EFF model was fit to the full subtracted profile and the structural parameters  $(\mu_0, \gamma, a)$  determined. This procedure includes an assumption that the central parameters  $(\mu_0, r_c)$  are essentially independent of the background level. We demonstrated the validity of this assumption, and indeed the entire background subtraction process in Paper I. In particular, it was shown that no significant systematic errors were introduced into the structural parameter measurements and especially the determination of  $\gamma$ , which is very sensitive to the background level.

Finally, uncertainties in the measured parameters  $(\mu_0, \gamma, a)$  were determined using a bootstrap method (Press et al. 1992, p691) with 1000 recursions, as described in Paper I.

**Table 3.** Structural parameters for the cluster sample derived from the best-fitting F555W EFF profiles.

Cluster Name	Centre (J2000.0) <sup>a</sup>		$\mu_{555}(0)$ <sup>b</sup>	$a$	$\gamma$	$r_c$	$r_c$	$r_m$
	$\alpha$	$\delta$		( $''$ )		( $''$ )	(pc) <sup>c</sup>	( $''$ )
NGC121	00 <sup>h</sup> 26 <sup>m</sup> 48 <sup>s</sup> .8	-71°32'12"	18.50 ± 0.06	12.97 ± 0.67	3.17 ± 0.08	9.61 ± 0.35	2.81 ± 0.10	76
NGC152	00 <sup>h</sup> 32 <sup>m</sup> 55 <sup>s</sup> .7	-73°07'01"	20.99 ± 0.04	20.24 ± 3.37	2.07 ± 0.26	19.74 ± 1.45	5.77 ± 0.42	76
NGC176	00 <sup>h</sup> 35 <sup>m</sup> 59 <sup>s</sup> .2	-73°09'59"	20.35 ± 0.08	10.21 ± 1.01	2.64 ± 0.14	8.49 ± 0.64	2.48 ± 0.19	64
NGC330	00 <sup>h</sup> 56 <sup>m</sup> 18 <sup>s</sup> .0	-72°27'47"	17.54 ± 0.05	10.58 ± 0.82	2.58 ± 0.14	8.93 ± 0.40	2.61 ± 0.12	72
NGC339	00 <sup>h</sup> 57 <sup>m</sup> 47 <sup>s</sup> .3	-74°28'22"	20.93 ± 0.06	45.73 ± 6.05	5.21 ± 0.99	25.26 ± 1.03	7.38 ± 0.30	72
NGC361	01 <sup>h</sup> 02 <sup>m</sup> 11 <sup>s</sup> .6	-71°36'21"	20.54 ± 0.05	18.49 ± 1.73	2.05 ± 0.13	18.17 ± 0.97	5.31 ± 0.28	76
NGC411	01 <sup>h</sup> 07 <sup>m</sup> 56 <sup>s</sup> .0	-71°46'03"	19.31 ± 0.04	11.93 ± 0.70	2.72 ± 0.11	9.72 ± 0.36	2.84 ± 0.11	76
NGC416	01 <sup>h</sup> 07 <sup>m</sup> 59 <sup>s</sup> .1	-72°21'12"	18.58 ± 0.05	14.42 ± 1.19	3.70 ± 0.32	9.73 ± 0.35	2.84 ± 0.10	72
NGC458	01 <sup>h</sup> 14 <sup>m</sup> 52 <sup>s</sup> .1	-71°33'05"	18.99 ± 0.08	15.03 ± 2.13	3.22 ± 0.34	11.02 ± 0.82	3.22 ± 0.24	69
KRON3	00 <sup>h</sup> 24 <sup>m</sup> 45 <sup>s</sup> .8	-72°47'38"	20.20 ± 0.03	26.97 ± 1.47	3.00 ± 0.14	20.67 ± 0.62	6.04 ± 0.18	76

<sup>a</sup> We find our centering algorithm to be repeatable to approximately  $\pm 1''$ , notwithstanding image header inaccuracies. Given this precision, coordinates in  $\delta$  are provided to the nearest arcsecond. Those in  $\alpha$  are reported to the nearest tenth of a second, but the reader should bear in mind that at  $\delta = -72^\circ$ , one second of RA corresponds to approximately five seconds of arc – in other words, the uncertainty in  $\alpha$  is approximately  $\pm 0^s.2$ .

<sup>b</sup> The  $V_{555}$  magnitude of one square arcsecond at the centre of a given cluster.

<sup>c</sup> When converting to parsecs we assume an SMC distance modulus of 18.9 which equates to a scale of 3.423 arcsec pc<sup>-1</sup>.

**Table 4.** Previously published core radius measurements.

Cluster	$r_c$ (pc)	$r_c$ (pc)	$r_c$ (pc)	Ratio <sup>c</sup>
	(this paper)	(published) <sup>a</sup>	(converted) <sup>b</sup>	
NGC121	2.81 ± 0.10	4.5	3.92	0.72
NGC152	5.77 ± 0.42	13.2	11.50	0.50
NGC176	2.48 ± 0.19	1.0	0.87	2.85
NGC330	2.61 ± 0.12	1.9	1.65	1.58
NGC339	7.38 ± 0.30	0.7	0.61	12.10
NGC361	5.31 ± 0.28	3.2	2.79	1.90
NGC411	2.84 ± 0.11	2.5	2.18	1.30
NGC416	2.84 ± 0.10	1.2	1.05	2.70
NGC458	3.22 ± 0.24	2.7	2.35	1.37
KRON3	6.04 ± 0.18	2.4	2.09	2.89

<sup>a</sup> Based on an SMC distance modulus of 19.2.

<sup>b</sup> Converted to our distance scale, with an SMC distance modulus of 18.9.

<sup>c</sup> Column 2 divided by Column 4.

## 4 RESULTS

### 4.1 Profiles and structural parameters

The background-subtracted F555W surface brightness profiles for each of the 10 clusters are presented in Fig. 1. To demonstrate the high degree of consistency between them, we plot each of the four annulus sets on the same axes. For each cluster, the best fit EFF profile is also plotted, the core radius indicated, and the best fit parameters listed. These results are summarized in Table 3 along with their corresponding errors, the calculated centre of each cluster and the maximum radial extent  $r_m$  of each profile's measurements.

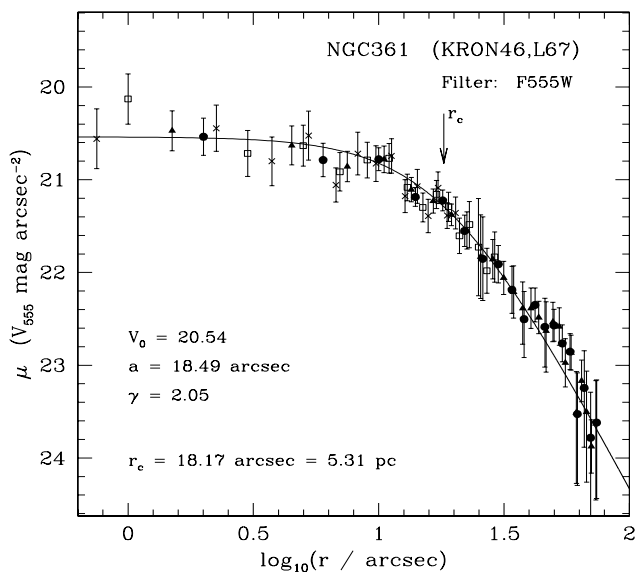
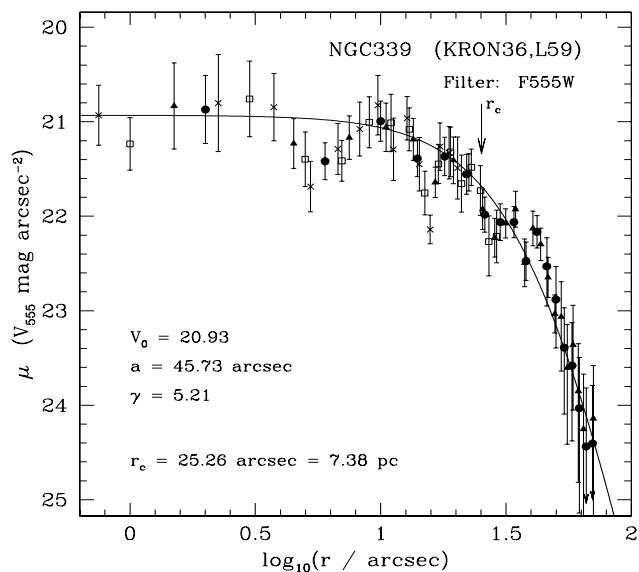
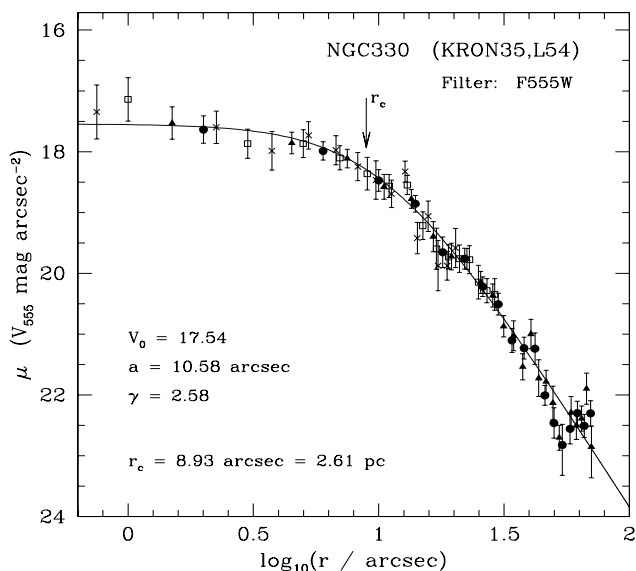
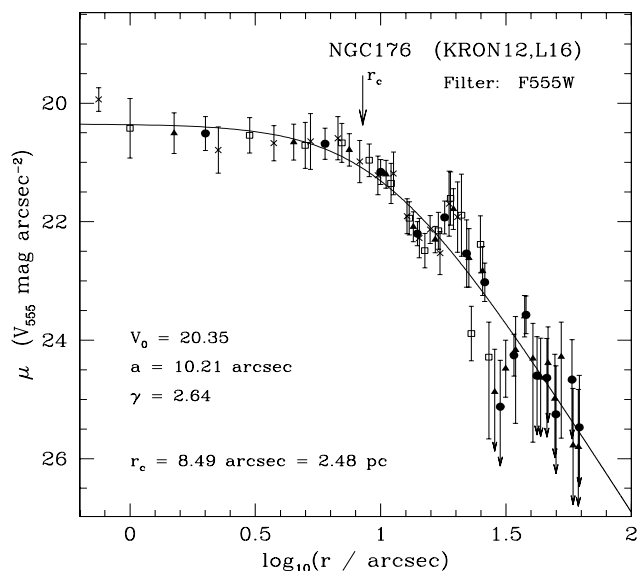
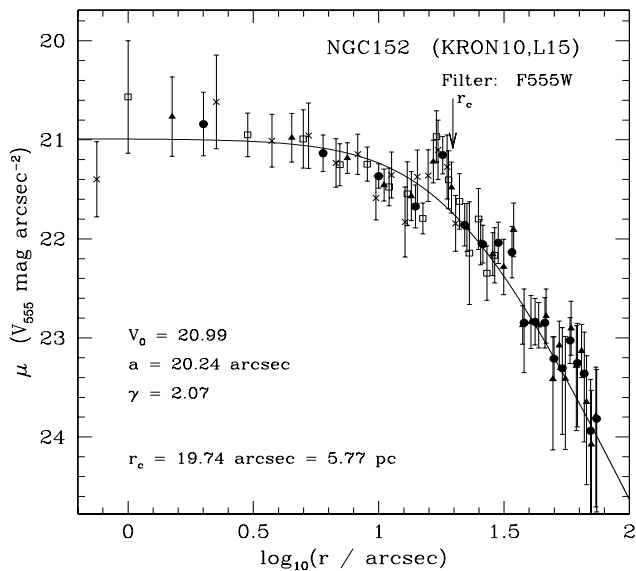
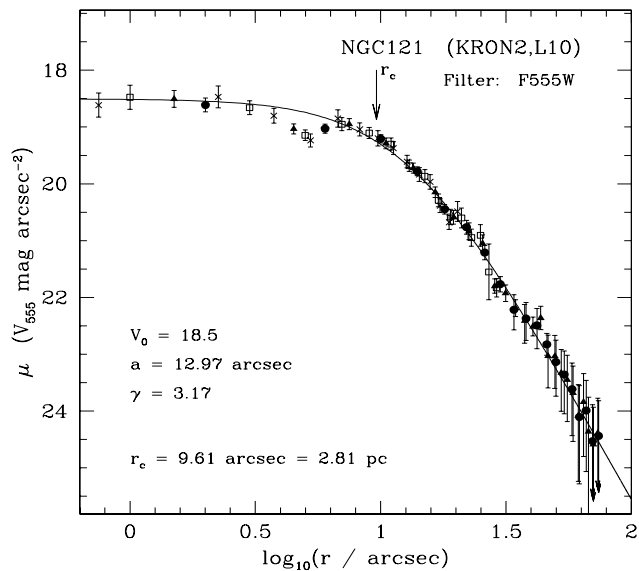
We have located only three published studies of SMC cluster profiles, all by the same authors – Kontizas, Danezis & Kontizas (1982) (20 clusters); Kontizas & Kontizas (1983) (23 clusters); and Kontizas, Theodosiou & Kontizas (1986) (24 clusters). The SMC cluster profiles presented in these papers are in fact density profiles from number counts off UK Schmidt plates, and so are not strictly comparable with our results. Nonetheless, we proceed for completeness. All ten of the clusters from our present sample are included in these works – five from the first paper listed above, and

five from the second. The values published in these papers are summarized in Table 4. For the purposes of comparison, we convert the published core radii to our distance scale<sup>†</sup>.

When the two sets of measurements are compared, we find significant discrepancies between them – nonetheless, these are expected and can be mostly accounted for. There appears to be both a systematic difference and large random differences present. Eight of our measured core radii are larger than the corresponding published radii; this systematic under-estimation is expected and is in fact predicted by the authors (Kontizas et al. 1982; Kontizas & Kontizas 1983). However, the degree of under-estimation is apparently not systematic, with our core radii ranging from 1.3 to  $\sim 12$  times larger than the published radii, suggesting significant random effects. Again, these errors might be expected, given the details of the photographic plate measurements. The authors report that their core radius estimates are derived from King models fitted to the density profiles, which yield  $r_t$  and the concentration  $c$ , with errors of  $\sim 15$  per cent in  $r_t$ . A similar random error in  $c$  could cause uncertainties of the order of  $\pm 60$  per cent or more in derived values of  $r_c$ , consistent with the difficulties associated with counting stars in crowded regions on photographic plates, and the resolution of the profiles (most do not extend within  $\sim 7$  pc). Such uncertainties would account for most of the observed scatter, and we therefore do not find any cause for alarm in the discrepancies we have reported, especially given the demonstrated success of our reduction procedure for the LMC cluster sample in Paper I.

Unlike for the LMC clusters, we do not observe any evidence for double or post core-collapse (PCC) clusters in the present sample. The lack of PCC clusters is not surprising – it is known that NGC 121, the oldest documented cluster in the SMC, is some 2 – 3 Gyr younger than the oldest LMC and Milky Way globular clusters (Mighell et al. 1998; Shara et al. 1998). It is therefore likely that no SMC clusters are dynamically old enough to have entered PCC evolution. The lack of double clusters, which are observed in abundance in the SMC (see e.g., the catalogue by de Oliveira et al. (2000b) and the references therein), can be ascribed to the small size of our sample. None of the clusters in the sample is present

<sup>†</sup> i.e., from the authors' adopted distance modulus of 19.2 to ours of 18.9



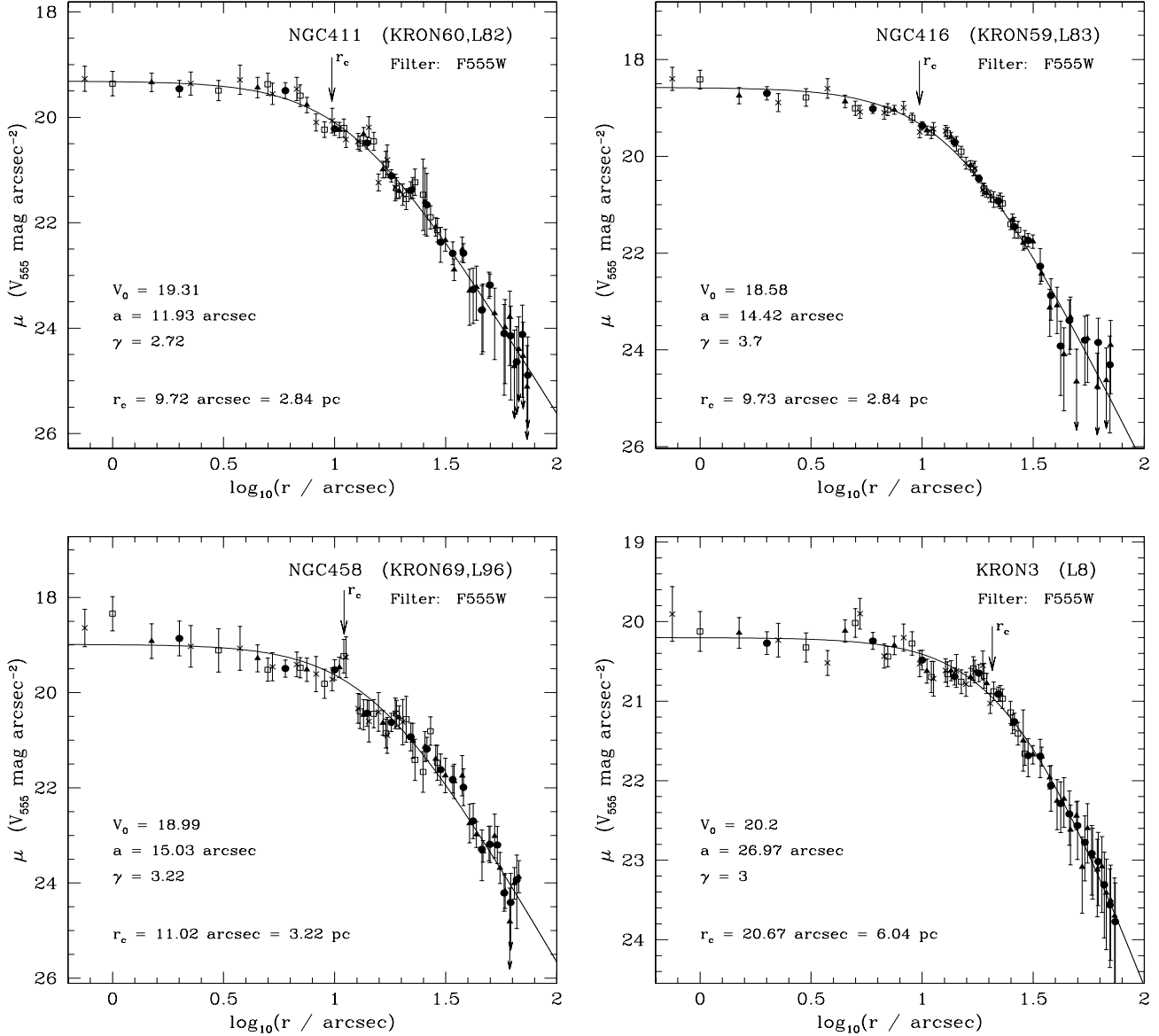


**Figure 1.** Background-subtracted F555W surface brightness profiles for each of the 10 clusters in the sample. The four different annulus widths are marked with different point types:  $1''.5$  width are crosses,  $2''$  width are open squares,  $3''$  width are filled triangles, and  $4''$  width are filled circles. Error bars marked with down-pointing arrows fall below the bottom of their plot. The solid lines show the best-fit EFF profiles. For each cluster the core radius  $r_c$  is indicated and the best-fit parameters listed. When converting to parsecs, we assume an SMC distance modulus of 18.9.

in the aforementioned catalogue. We note, however, the presence of a bump in the profile of NGC 152, and a bump at lower significance in the profile of NGC 176. These bumps are reminiscent of those observed for the LMC clusters NGC 2213 and NGC 2153 (see Paper I), albeit not as prominent. Just as with the LMC clusters, the causes of the bumps are not yet clear and it is uncertain as to whether any physical significance can be attached to them. The images of these clusters show that there are certainly no evident sub clusters like NGC 1850B in the LMC.

## 4.2 Luminosity and mass estimates

We can use the structural parameters obtained from the surface brightness profiles to estimate luminosities and masses for each

cluster, and the procedure for this is described at length in Paper I. We showed that for a cluster with a profile given by Eq. 2, the asymptotic luminosity is given by:

$$L_\infty = \frac{2\pi\mu_0 a^2}{\gamma - 2} \quad (5)$$

provided  $\gamma > 2$ . In cases where  $\gamma \approx 2$ , this value may become unreasonably large and the limit  $r \rightarrow \infty$  may not be justified. We therefore provided a lower-limit estimate,  $L_m$ , which is the enclosed luminosity within a cylinder of radius  $r_m$  along the line of sight, where  $r_m$  is the maximum radial extent measured for a given profile (see Table 3):

$$L_m = \frac{2\pi\mu_0}{\gamma - 2} \left( a^2 - a^\gamma (a^2 + r_m^2)^{-\frac{(\gamma-2)}{2}} \right) \quad (6)$$

**Table 5.** Luminosity and mass estimates calculated using the structural parameters from the best fitting EFF profiles.

Cluster	$\log \mu_0^a$ ( $L_\odot \text{ pc}^{-2}$ )	Adopted [Fe/H]	Adopted $M/L_V$	$\log j_0$ ( $L_\odot \text{ pc}^{-3}$ )	$\log L_\infty$ ( $L_\odot$ )	$\log L_m$ ( $L_\odot$ )	$\log \rho_0$ ( $M_\odot \text{ pc}^{-3}$ )	$\log M_\infty$ ( $M_\odot$ )	$\log M_m$ ( $M_\odot$ )
NGC121	$3.23 \pm 0.02$	-1.65	2.74	$2.47 \pm 0.05$	$5.12 \pm 0.10$	$5.06 \pm 0.08$	$2.91 \pm 0.05$	$5.55 \pm 0.10$	$5.50 \pm 0.08$
NGC152	$2.23 \pm 0.02$	-0.64	0.63	$1.17^{+0.13}_{-0.12}$	$5.73^{+0.52}_{-0.85}$	$4.69^{+0.18}_{-0.21}$	$0.97^{+0.13}_{-0.12}$	$5.53^{+0.52}_{-0.85}$	$4.49^{+0.18}_{-0.21}$
NGC176	$2.49 \pm 0.03$	-0.64	0.23	$1.79 \pm 0.09$	$4.43^{+0.22}_{-0.21}$	$4.27^{+0.14}_{-0.15}$	$1.15 \pm 0.09$	$3.79^{+0.22}_{-0.21}$	$3.63^{+0.14}_{-0.15}$
NGC330	$3.61 \pm 0.02$	-0.64	0.09	$2.89 \pm 0.07$	$5.63^{+0.20}_{-0.18}$	$5.46^{+0.12}_{-0.13}$	$1.84 \pm 0.07$	$4.58^{+0.20}_{-0.18}$	$4.41^{+0.12}_{-0.13}$
NGC339	$2.26 \pm 0.02$	-1.65	1.66	$1.07 \pm 0.13$	$4.80^{+0.29}_{-0.26}$	$4.74^{+0.19}_{-0.22}$	$1.29 \pm 0.13$	$5.02^{+0.29}_{-0.26}$	$4.96^{+0.19}_{-0.22}$
NGC361	$2.41 \pm 0.02$	-1.65	2.03	$1.39 \pm 0.08$	$5.98^{+0.46}_{-0.66}$	$4.82^{+0.11}_{-0.12}$	$1.70 \pm 0.08$	$6.29^{+0.46}_{-0.66}$	$5.13^{+0.11}_{-0.12}$
NGC411	$2.91 \pm 0.02$	-0.64	0.63	$2.14 \pm 0.05$	$4.93^{+0.14}_{-0.13}$	$4.80 \pm 0.10$	$1.94 \pm 0.05$	$4.73^{+0.14}_{-0.13}$	$4.60 \pm 0.10$
NGC416	$3.20 \pm 0.02$	-1.65	1.79	$2.43 \pm 0.08$	$5.02^{+0.18}_{-0.17}$	$4.99 \pm 0.15$	$2.68 \pm 0.08$	$5.27^{+0.18}_{-0.17}$	$5.24 \pm 0.15$
NGC458	$3.03 \pm 0.03$	-0.33	0.25	$2.21 \pm 0.12$	$5.03^{+0.29}_{-0.27}$	$4.96^{+0.21}_{-0.23}$	$1.61 \pm 0.12$	$4.43^{+0.29}_{-0.27}$	$4.36^{+0.21}_{-0.23}$
KRON3	$2.55 \pm 0.01$	-1.65	1.60	$1.46 \pm 0.05$	$5.14 \pm 0.12$	$4.97^{+0.07}_{-0.08}$	$1.66 \pm 0.05$	$5.35 \pm 0.12$	$5.17^{+0.07}_{-0.08}$

<sup>a</sup> Corrected for reddening using  $E(B - V) = 0.05$  (see text).

We obtain the central surface brightness  $\mu_0$  in units of  $L_\odot \text{ pc}^{-2}$  by using the relation from Paper I, that:

$$\log \mu_0 = 0.4(V_{555}^\odot - \mu_{555}(0) + DM + 3.1E(B - V)) + \log(3.423^2) L_\odot \text{ pc}^{-2} \quad (7)$$

It was shown in Paper I that  $V_{555}^\odot = +4.85$  is an appropriate value for the F555W absolute solar magnitude. We assume a uniform reddening of  $E(B - V) = 0.05$ , which is a reasonable approximation in the direction of the SMC (see e.g., the values given in Table 2 of Crowl et al. (2001)), and an SMC distance modulus of 18.9, which is where the factor  $3.423 \text{ arcsec pc}^{-1}$  arises from.

Estimates for the masses  $M_\infty$  and  $M_m$ , and the central density  $\rho_0$ , which correspond to  $L_\infty$ ,  $L_m$  and  $j_0$  respectively, are obtained by multiplying the appropriate equation by the mass to light ratio  $M/L_V$  for the cluster in question. To obtain estimates of these ratios, we use the evolutionary synthesis code of Fioc & Rocca-Volmerange (1997) (PEGASE v2.0, 1999), which determines the integrated properties of a synthetic stellar population as a function of time. We adopted the simplest possible model - a population of stars formed simultaneously in one initial burst and with the same metallicity - presumably a fairly good approximation to the formation of a rich stellar cluster. For the initial mass function (IMF), we used that of Kroupa, Tout & Gilmore (1993) over the mass range 0.1 to  $120M_\odot$ . There are four available abundances for these calculations ([Fe/H]  $\approx -2.25, -1.65, -0.64$ , and  $-0.33$ ) and we adopted the most suitable one for a given cluster based on the literature estimates in Table 2. As shown in Paper I, these calculations are relatively insensitive to the chosen metallicity - in fact it is sufficient to determine whether a cluster is metal rich ([Fe/H]  $\approx -0.33$ ) or metal poor ([Fe/H]  $\approx -2.25$ ) - and we are therefore confident in using even those metallicities from Table 2 which are not particularly well constrained.

The mass, luminosity and density values calculated for the SMC cluster sample are presented in Table 5. Just as for the LMC sample, the indicated errors reflect the random uncertainties due to the parameters ( $\mu_0, \gamma, a$ ) and do not include the systematic uncertainties which might be introduced through the mass to light ratios, or by the observation techniques (such as the loss of luminosity/mass due to saturated stars). Such systematics are not expected to be unreasonably large - as discussed in Paper I, they should be within the random errors.

## 5 THE CORE RADIUS VS. AGE RELATIONSHIP

In Paper I, evidence for a trend in core radius with age for the LMC cluster system was presented - namely that the spread in cluster core radius increases with increasing age. This trend was discussed in detail, and the argument made that the relationship represents true physical evolution in these clusters. One of the first things we would like to ask for the present sample is whether such a relationship is also present for the SMC cluster system, and if so whether it is noticeably different in any way from that observed in the LMC.

We have plotted core radius against age for the ten clusters, in Figure 2(a). Even though our sample is small and therefore incomplete, it immediately seems that the same trend in core radius exists for the SMC cluster system. This is the first time that this has been shown for SMC clusters. The youngest clusters have relatively compact cores, whereas the older clusters can have either compact cores or much larger cores. The similarity of the SMC cluster trend to that for the LMC sample is evident when the data for both systems are over-plotted (Figure 2(b)). Aside from the fact that four of the SMC clusters fall in the LMC cluster age gap, no significant differences between the two relationships can be claimed, at least within the limits of the current data. Both plots show a bifurcation at approximately several  $\times 10^8$  yr, with the majority of clusters following the lower sequence in the diagram, but with some clusters moving to the upper right. The two pairs of sequences fall nicely on top of each other. If anything, the SMC clusters on the lower sequence have slightly larger core radii on average than the LMC lower sequence clusters; however, this could be due to uncertainties in both the SMC distance modulus and line-of-sight spatial depth. It is tempting to suggest that a larger fraction of SMC clusters than LMC clusters evolve to the upper sequence, but given the small size of the SMC sample, we cannot claim this without additional data.

In Paper I, we used two diagnostic plots -  $M_\infty$  vs.  $\log \tau$  and  $M_\infty$  vs.  $r_c$  - to show that the radius-age relationship is not due to a correlation between mass and age, and mass and core radius. We can use the current data both to demonstrate this for the SMC clusters, and also to search for any systematic differences which might be present between the two cluster systems and which might help shed light on the core radius vs. age trend. The two diagnostic plots are presented in Fig. 3(a) and Fig. 4(a) respectively. The LMC data is added to these diagrams in Fig. 3(b) and Fig. 4(b).

Fig. 3(a) shows the possibility of a slight correlation of SMC cluster mass with age; however this apparent correlation is proba-



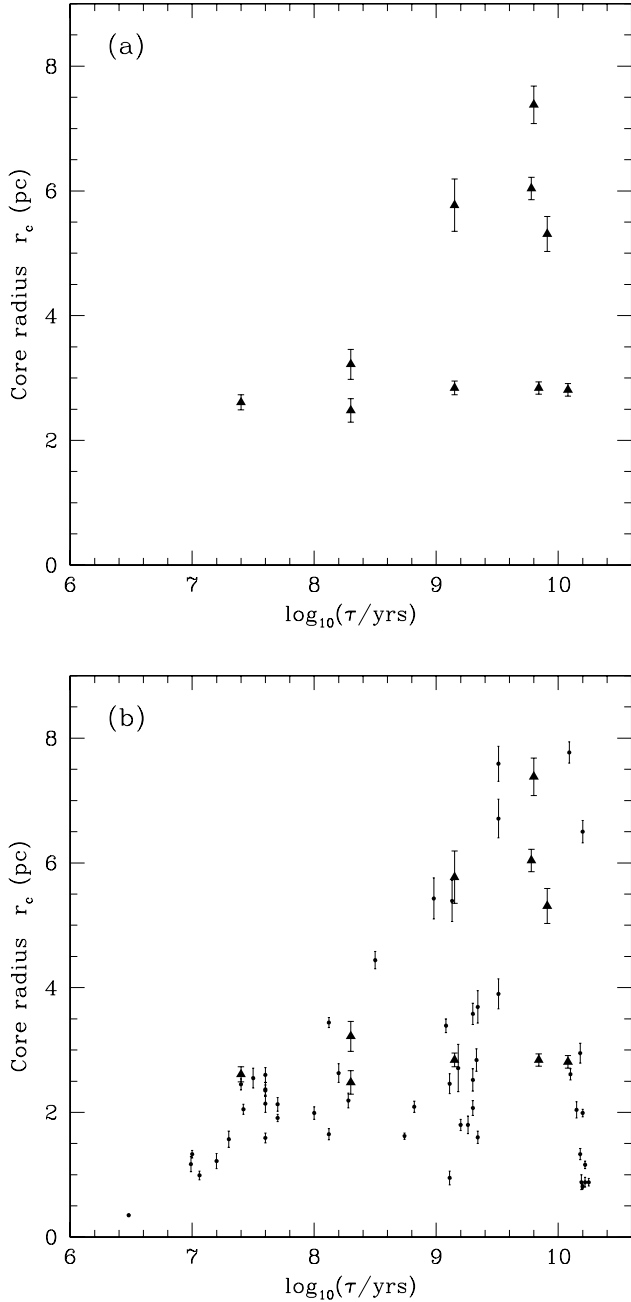


**Figure 2.** Core radius vs. age for (a) all ten SMC clusters and (b) SMC clusters (solid large triangles) and LMC clusters (small solid circles) together. Data for the SMC cluster ages are from Table 2 and core radii from Table 3; all LMC cluster data is from Paper I.

ably due to the incompleteness of the sample, particularly for clusters younger than  $10^9$  yr. When compared with the LMC sample, which showed no such correlation, the agreement is close. The lowest mass SMC cluster is not of unusually low mass; similarly, the highest mass cluster is not overly massive. In fact, without the addition of more SMC clusters to the sample, the plots for the two systems cannot be considered to show any significant differences. The same result applies for the plot of  $M_\infty$  against  $r_c$ . No correlation is evident from the SMC data alone, and there are no significant differences between the SMC and LMC data – in fact, the agreement

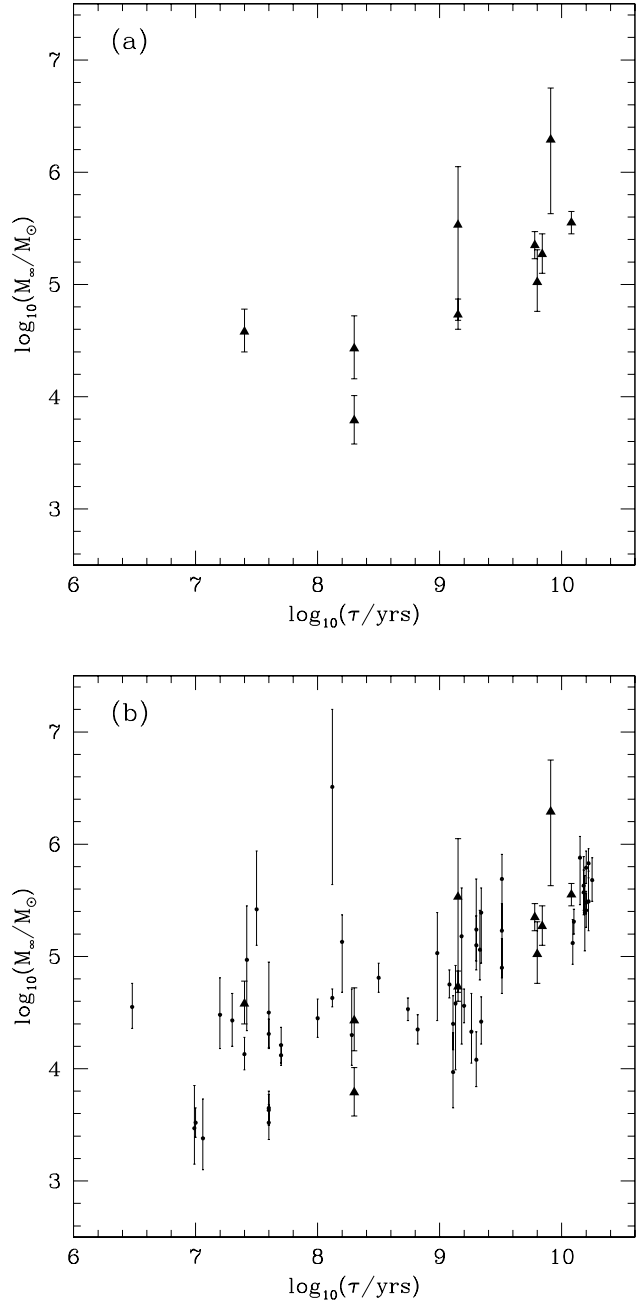


**Figure 3.** Asymptotic mass vs. age for (a) all ten SMC clusters and (b) SMC clusters (solid large triangles) and LMC clusters (small solid circles) together. Data for the SMC cluster ages are from Table 2 and masses from Table 5; all LMC cluster data is from Paper I.

is extremely close. This further strengthens both the conclusion that there is little difference between the core radius vs. age relationship for each system, and that this relationship represents real evolution in the structure of clusters as they grow older. Furthermore, if the suggestion that a higher fraction of SMC than LMC clusters have expanded cores *does* hold true given more data, this is unlikely to be due to significantly different cluster mass distributions between the two systems.

The apparent close agreement between the structural parameters of the LMC and SMC clusters is potentially significant given

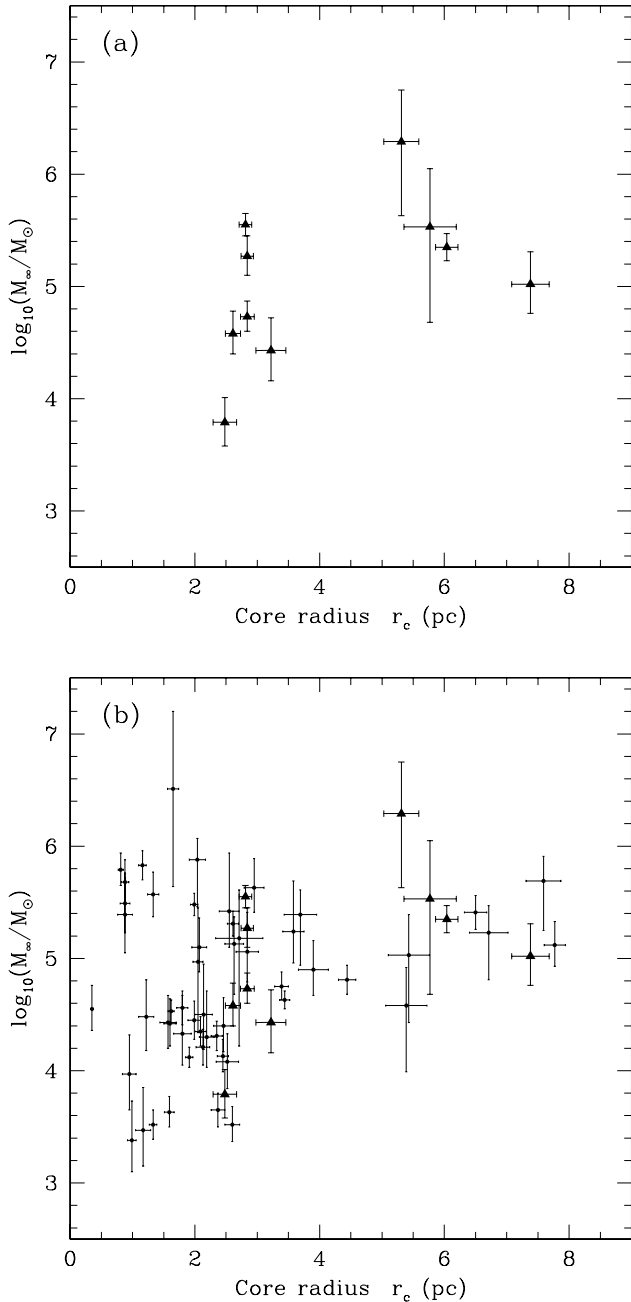


**Figure 4.** Asymptotic mass vs. core radius for (a) all ten SMC clusters and (b) SMC clusters (solid large triangles) and LMC clusters (small solid circles) together. Data for the SMC cluster core radii are from Table 3 and masses from Table 5; all LMC cluster data is from Paper I.

that the two systems are known to exhibit strong differences in other aspects. The LMC apparently started forming globular clusters some 2 – 3 Gyr before the SMC, as evidenced by the age ( $11.9 \pm 1.3$  Gyr) of the oldest known SMC cluster, NGC 121 (Mighell et al. 1998), compared with the ages ( $\sim 16 \pm 3$  Gyr) of the oldest LMC clusters (Olsen et al. (1998); see also Shara et al. (1998)). Furthermore, the LMC seems to have had a long quiescent period in cluster formation, with only one cluster (ESO 121-SC03) definitely within the so called “age gap” between  $\sim 3 - 12$  Gyr (see e.g. Rich, Shara & Zurek (2001) and references therein). The SMC

on the other hand, continued forming clusters during this period, possessing at least seven with ages lying in the age gap range (see e.g., Mighell et al. (1998)). The age-metallicity relationships for the two systems are correspondingly different – the LMC possesses an abundance gap which matches the age gap (again see e.g., Rich et al. (2001)) but appears to have undergone considerable chemical enrichment during this period (Mighell et al. 1998). For a detailed discussion of this, we refer the reader to the study of Gilmore & Wyse (1991) who investigate the chemical evolution of systems which undergo bursts of star formation, with particular application to the LMC. In contrast with the LMC, the SMC has plenty of intermediate metallicity clusters (see e.g., Da Costa & Hatzidimitriou (1998)) and does not seem to have undergone such a steep chemical enrichment in the age gap period. The data of Mighell et al. suggest that a bursting model of star formation might best fit the SMC age-metallicity relation, with a 2 Gyr peak of formation around 11 Gyr ago, then a lower but constant formation rate until  $\sim 2$  Gyr ago. Da Costa & Hatzidimitriou suggest a closed box model of chemical enrichment best fits their (slightly different) spectroscopic metallicity determinations.

It is intriguing that two systems with such evidently disparate cluster formation histories should nonetheless possess cluster systems which appear to have followed such similar evolutionary paths. This again reinforces the idea that the trend in core radius with age observed for both systems is purely a result of some aspect of cluster evolution; an aspect which should operate similarly in each of the two Magellanic Clouds. The need for additional data is clear and paramount, and the acquisition of this data is a crucial part of the future development of this work. *N*-body simulations are also underway (e.g., Wilkinson et al., in prep.), exploring how different stellar populations, and external influences such as those described in Paper I can affect the evolution of cluster cores.

## 6 SUMMARY AND CONCLUSIONS

In a follow-up to our recent work detailing the structures of a large sample of LMC clusters (Paper I), we have obtained a similar archival *HST* snapshot data set for a sample of ten SMC clusters. We have constructed surface brightness profiles for these clusters, and obtained measurements of their structural parameters, following a method exactly similar to that applied to the LMC sample. Luminosities, masses and central densities have also been estimated for the SMC sample. These data, along with the surface brightness profiles, are available on-line at [http://www.ast.cam.ac.uk/STELLARPOPS/SMC\\_clusters/](http://www.ast.cam.ac.uk/STELLARPOPS/SMC_clusters/). Unlike for the LMC sample, we do not see any evidence for post core-collapse clusters in our sample, but this is not unexpected. Similarly, we do not see any compelling evidence from the surface brightness profiles for double clusters in our sample, although a couple of profiles show bumps similar to those observed for several LMC clusters.

We have used our core radius measurements for the SMC sample to investigate further the core radius vs. age relationship, which was described in detail in Paper I. Although compromised somewhat by the small sample size, our analysis shows that the SMC clusters apparently follow a very similar relationship to the LMC clusters, with some clusters maintaining small cores throughout their lives, but with others developing much enlarged cores. It is possible that a higher percentage of rich SMC clusters than rich LMC clusters develop such expanded cores. Additional data, both

observational and computational, is required to further explore this relationship and the physical processes involved.

## ACKNOWLEDGMENTS

ADM would like to acknowledge the support of a Trinity College ERS grant and a British government ORS award. This paper is based on observations made with the NASA/ESA *Hubble Space Telescope*, obtained from the data archive at the Space Telescope Institute. STScI is operated by the association of Universities for Research in Astronomy, Inc. under the NASA contract NAS 5-26555.

## REFERENCES

- Alves D., Sarajedini A., 1999, *ApJ*, 511, 225
- Chiosi C., Vallenari A., Bressan A., Deng L., Ortolani S., 1995, *A&A*, 293, 710
- Crowl H. H., Sarajedini A., Piatti A. E., Geisler D., Bica E., Clariá J. J., Santos Jr. J. F. C., 2001, *AJ*, 122, 220
- Da Costa G. S., Hatzidimitriou D., 1998, *AJ*, 115, 1934
- de Oliveira M. R., Dutra C. M., Bica E., Dottori H., 2000b, *A&AS*, 146, 57
- Djorgovski S., 1987, in Grindlay J., Philip A. G. D., eds, *Proc. IAU Symp.* 126, *Globular Cluster Systems in Galaxies*. Kluwer, Dordrecht, p. 333
- Dolphin A. E., 2000a, *PASP*, 112, 1383
- Dolphin A. E., 2000b, *PASP*, 112, 1397
- Elson R. A. W., 1991, *ApJS*, 76, 185
- Elson R. A. W., 1992, *MNRAS*, 256, 515
- Elson R. A. W., Fall S. M., Freeman K. C., 1987, *ApJ*, 323, 54
- Elson R. A. W., Freeman, K. C., Lauer, T. R., 1989, *ApJ*, 347, L69
- Fioc M., Rocca-Volmerange B., 1997, *A&A*, 326, 950
- Gilmore G., Wyse R. F. G., 1991, *ApJ*, 367, L55
- Hill V., 1999, *A&A*, 345, 430
- Hodge P., Flower P., 1987, *PASP*, 99, 734
- King I., *AJ*, 1962, 67, 471
- Kontizas E., Kontizas M., 1983, *A&AS*, 52, 143
- Kontizas M., Danezis E., Kontizas E., 1982, *A&AS*, 49, 1
- Kontizas M., Theodosiou E., Kontizas E., 1986, *A&AS*, 65, 207
- Kron G. E., 1956, *PASP*, 68, 125
- Kroupa P., Tout C. A., Gilmore G. F., 1993, *MNRAS*, 262, 545
- Lindsay E. M., 1958, *MNRAS*, 118, 172
- Mackey A. D., Gilmore G. F., 2002, *MNRAS*, submitted (Paper I)
- Mighell K. J., Sarajedini A., French R. S., 1998, *AJ*, 116, 2395
- Olsen K. A. G., Hodge P. W., Mateo M., Olszewski E. W., Schommer R. A., Suntzeff N. B., Walker A. R., 1998, *MNRAS*, 300, 665
- Press W. H., Teukolsky S. A., Vetterling W. T., Flannerty B. P., 1992, *Numerical Recipes in C: The Art of Scientific Computing*, (2nd Edition). Cambridge University Press, New York
- Rich R. M., Shara M. S., Fall M., Zurek D., 2000, *AJ*, 119, 197
- Rich R. M., Shara M. M., Zurek D., 2001, *AJ*, 122, 842
- Shara M. M., Fall S. M., Rich R. M., Zurek D., 1998, *ApJ*, 508, 570
- Welch D. L., 1991, *AJ*, 101, 538
- Westerlund B. E., 1997, *The Magellanic Clouds*. Cambridge University Press, Cambridge

This paper has been produced using the Royal Astronomical Society/Blackwell Science  $\LaTeX$  style file.